Proceedings of the 13th
KACC, October 1998

Vibration Control of Aerial Vehicles in the Derricking Action

Katsunobu KONISHI, Hiroyuki UKIDA, and Isamu UCHIHARA

Department of Mechanical Engineering, Tokushima University
2-1, Minami-Josanjima, Tokushima, 770, Japan
Tel : 81-886-56-7383
Fax : 81-886-56-9082
Email : konishi@me.tokushima-u.ac.jp

Abstract

This paper presents a scheme to actively control the vertical vibration of aerial vehicles due to the disturbances such as the sudden change of derricking angle and the external forces by using a small plunger attached to the derricking cylinder. Simulations show that the 1st mode vibration is suppressed efficiently by the proposed method without exciting the higher modes' vibration. Detailed mathematical model of the aerial vehicle, its vibration characteristics, detection method of the 1st mode vibration and the controller design based on the lag-element and the disturbance observer are described.

1. Introduction

Recently, many robotized manipulator system[1] for live-line maintenance work are used to avoid the risk of electrical shock, the danger of falling from a high place, the requirement of heavy labor and so on.

However, the efficiency of the system is not so high compared with the direct hot-line work using rubber-insulated gloves because the manipulator itself vibrates together with the bucket and boom due to the disturbance forces such as the inertial force caused by the position change, the wind force, and the reaction force of the manipulator. Therefore, it is necessary to suppress the vibration of the bucket by using an appropriate actuator.

Fig.1 shows the schematic diagram of the aerial vehicle treated in this paper. Since the main component of the aerial vehicles vibration is the 1st mode vibration, the translation of the bucket is much superior to its rotation. Therefore, it is needed to give the bucket the translation motion in order to suppress its vibration. From this reason, two schemes seem to be possible. One is to move the bucket relatively to the boom by using a guide rail and a hydraulic actuator attached at the top of the boom. Although the effectiveness of this scheme was confirmed by various simulations in ref.[2], it is not always suitable for the practical use because it requires the extra weight mounted on the boom. By the way, the usage of the upper leveling cylinder will not efficient because it hardly gives the translation motion to the bucket.

Another scheme is to control the hydraulic pressure of the derricking cylinder. Although this scheme has a disadvantage that the higher modes' vibration may be excited, it dose not need extra equipment. Therefore, it is easy to apply to the practical aerial vehicles if its controller is sufficiently simple and stable. From this point of view, (i) detailed mathematical model for the aerial vehicle to simulate its vibration precisely, (ii) vibration characteristics, and (iii) a simple controller for the 1st mode vibration, are presented in this paper.

2. Vibration Model

In this section, the vibration model for aerial vehicles is proposed based on the model defined by Fig.1~Fig.3. The model is constructed by using the following assumptions; (H1) the carrier and the rotary frame are a rigid body suspended by four springs which are the approximation of the outriggers, (H2) the bucket is rigid, (H3) the hydraulic cylinders are elastic due to the compressibility of the working oil, (H4) the boom deflection is approximated by the well known beam element for the middle span of each stage, and it bends by an angles ϕ at the mid-point (B_i in Fig.3) of the overlap region of the neighboring stages.

This model becomes more precise than the previous models[3],[4] for cranes. The variables including in the model are

$$\boldsymbol{q} = \left[x, z, \alpha, \beta, \eta_1, \theta_1, \phi_1, \eta_2, \theta_2, \phi_2, \eta_3, \theta_3, \phi_3, \eta_4, \theta_4, \gamma\right]^T \quad (1)$$

If the gravity acceleration g is assumed to be zero and there is no vibration, $\boldsymbol{q}$ becomes

$$\boldsymbol{q}^* = \left[0, 0, 0, \beta^*, 0, 0, 0, 0, 0, 0, 0, 0, 0, 0, \gamma^*\right]^T \quad (2)$$

where β^* is the angle determined by the volume of the working oil in the derricking cylinder, and γ^* is well approximated by $90° - \beta^*$ by the interaction between the lower and upper leveling cylinders. In this paper, β^* is used as the reference quantity instead of the volume of working oil.

3. Equations of motion

3.1 Mechanical energies

Let T, U and V be kinetic energy, elastic energy and potential energy. These energies of the total system of aerial vehicle are given by

$$\left.\begin{aligned} T &= T_{CR} + T_{BM} + T_{BT} \\ U &= U_{CR} + U_{BM} + U_{DC} + U_{LC} \\ V &= V_{CR} + V_{BM} + V_{BT} \end{aligned}\right\} \quad (3)$$

where subscripts CR, BM, BT, DC and LC denote the carrier and the rotary frame, the boom, the bucket, the derricking cylinder and the upper leveling cylinder. The outline of each energy becomes as follows.

(A) Carrier and rotary frame :

$$\left.\begin{aligned} T_{CR} &= \frac{1}{2}m_{G1}\left[\left(\dot{x}+h_{G1}\dot{\alpha}\right)^2+\left(\dot{z}-l_{G1}\dot{\alpha}\right)^2\right]+\frac{1}{2}J_{G1}\dot{\alpha}^2 \\ U_{CR} &= \frac{1}{2}\left(k_{H1}+k_{H2}\right)x^2+\frac{1}{2}k_{V1}\left(z+l_{A1}\alpha\right)^2 \\ &\quad +\frac{1}{2}k_{V2}\left(z-l_{A2}\alpha\right)^2 \\ V_{CR} &= m_{G1}g\left(h_{G1}+z-l_{G1}\alpha\right) \end{aligned}\right\} \quad (4)$$

(B) Boom :

$$\left.\begin{aligned} T_{BM} &= \sum_{i=1}^{4}\frac{1}{2}\left(N_{i1}v^2+\boldsymbol{P}_{i1}{}^T\boldsymbol{R}_{i1}\boldsymbol{P}_{i1}\right) \\ U_{BM} &= \sum_{i=1}^{4}\frac{1}{2}\left(k_{i-1}\phi_{i-1}{}^2+\boldsymbol{P}_{i2}{}^T\boldsymbol{R}_{i2}\boldsymbol{P}_{i2}\right),\ \ \phi_0=0 \\ V_{BM} &= \sum_{i=1}^{4}g\left(N_{i1}z_{B0}-\boldsymbol{P}_{i2}{}^T\boldsymbol{R}_{i3}\sin\lambda+N_{i2}\cos\lambda\right) \end{aligned}\right\} \quad (5)$$

where $\lambda=\alpha+\beta$, N_{i1} is the mass of the ith boom, v is the velocity of the boom in the ξ direction, z_{B0} is the z coordinate of the point B_0, N_{i2} is the mass moment of the ith boom with respect to the point B_0. The second term of the right-hand side of each energy is the energy when the displacement η at the mid-part $B_{i-1}B_i$ of the ith boom is approximated by the beam element as follows.

$$\eta=f_1\left(\bar{\xi}\right)\eta_{i-1}+f_2\left(\bar{\xi}\right)\left(\theta_{i-1}+\phi_{i-1}\right)+f_3\left(\bar{\xi}\right)\eta_i+f_4\left(\bar{\xi}\right)\theta_i \quad (6)$$

$$\left.\begin{aligned} f_1\left(\bar{\xi}\right) &= 1-3\bar{\xi}^2+2\bar{\xi}^3 \\ f_2\left(\bar{\xi}\right) &= \left(\bar{\xi}-2\bar{\xi}^2+\bar{\xi}^3\right)l_i \\ f_3\left(\bar{\xi}\right) &= 3\bar{\xi}^2-2\bar{\xi}^3 \\ f_4\left(\bar{\xi}\right) &= \left(-\bar{\xi}^2+\bar{\xi}^3\right)l_i,\quad \bar{\xi}=\left(\xi-L_{i-1}\right)/l_i \end{aligned}\right\} \quad (7)$$

$\boldsymbol{R}_{i1}\sim\boldsymbol{R}_{i3}$ are constant matrices, $\boldsymbol{P}_{i1}$ and $\boldsymbol{P}_{i2}$ are given by

$$\left.\begin{aligned} \mathbf{P}_{i1} &= \left[\dot{\eta}_{i-1}+w_{i-1},\ \dot{\theta}_{i-1}+\dot{\phi}_{i-1}+\dot{\lambda},\ \dot{\eta}_i+w_i,\ \dot{\theta}_i+\dot{\lambda}\right]^T \\ \boldsymbol{P}_{i2} &= \left[\eta_{i-1},\ \theta_{i-1}+\phi_{i-1},\ \eta_i,\ \theta_i\right]^T \end{aligned}\right\} \quad (8)$$

where w_i denotes the velocity of the point D_i in the η direction in Fig.3.

(C) Bucket :

$$\left.\begin{aligned} T_{BT} &= \frac{1}{2}\left[m_{G2}\left(v_{G2}{}^2+w_{G2}{}^2\right)+J_{G2}\dot{\psi}^2\right] \\ V_{BT} &= m_{G2}g\left[z_{B0}+\left(b_6-\eta_4-l_5\theta_4\right)\sin\lambda\right. \\ &\quad \left.+\left(L_4+l_5+b_6\theta_4\right)\cos\lambda+h_{G2}\cos\psi-l_{G2}\sin\psi\ \right] \end{aligned}\right\} \quad (9)$$

where $\psi=\alpha+\beta+\theta_4+\gamma-\pi/2$, v_{G2} and w_{G2} denote the velocities of G_2 in the ξ and η directions, respectively. Since the bucket is rigid, $U_{BT}=0$.

(D) Derricking cylinder :

$$U_{DC}=\frac{1}{2}k_{DC}\left[d_{DC}\left(\beta-\beta^*\right)+\eta_{G2}\sin\sigma^*+\frac{A_{PLG}}{A_{DC}}u\right]^2 \quad (10)$$

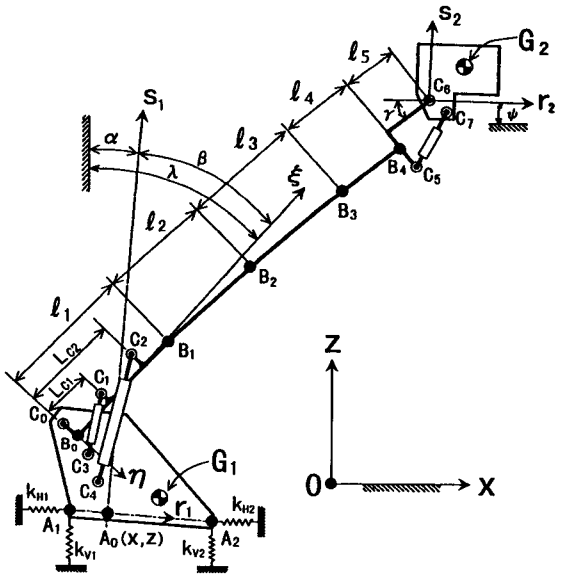

Fig.1 Schematic diagram of the aerial vehicle

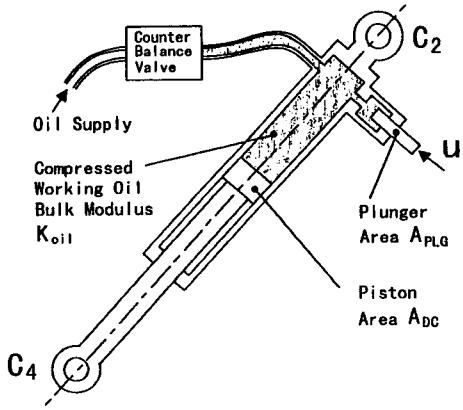

Fig.2 Derricking cylinder and planger

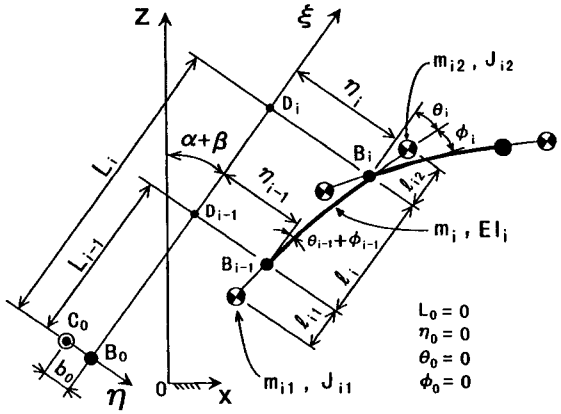

Fig.3 Deflection of the boom

Table1 Parameters of the aerial vehicle

Carrier and Rotary Frame							
m_{G1}	(kg)	5510	ℓ_{G1}	(m)	0.37	h_{G1}	(m)	0.07
J_{G1}	(kgm²)	3500	ℓ_{A1}	(m)	0.19	h_{A1}	(m)	0
K_{H1}	(N/m)	1.8E+6	ℓ_{A2}	(m)	2.66	h_{A2}	(m)	0
K_{H2}	(N/m)	1.8E+6	ℓ_{C0}	(m)	0.65	h_{C0}	(m)	2.01
K_{V1}	(N/m)	2.4E+6	ℓ_{C3}	(m)	0.50	h_{C3}	(m)	1.85
K_{V2}	(N/m)	2.4E+6	ℓ_{C4}	(m)	0.13	h_{C4}	(m)	1.45
Boom								
m_1	(kg)	300	J_{32}	(kgm²)	0.7	L_{C2}	(m)	2.15
m_{11}	(kg)	51	J_{41}	(kgm²)	0.1	L_1	(m)	2.41
m_{12}	(kg)	70	J_{42}	(kgm²)	6.3	L_2	(m)	5.09
m_2	(kg)	177	ℓ_1	(m)	2.41	L_3	(m)	7.82
m_{21}	(kg)	27	ℓ_{11}	(m)	0.21	L_4	(m)	10.19
m_{22}	(kg)	41	ℓ_{12}	(m)	0.21	b_0	(m)	0.25
m_3	(kg)	123	ℓ_2	(m)	2.68	b_1	(m)	0.27
m_{31}	(kg)	13	ℓ_{21}	(m)	0.21	b_2	(m)	0.31
m_{32}	(kg)	39	ℓ_{22}	(m)	0.15	b_5	(m)	0.03
m_4	(kg)	86	ℓ_3	(m)	2.73	b_6	(m)	0.18
m_{41}	(kg)	8	ℓ_{31}	(m)	0.15	EI_1	(Nm²)	2.9E+7
m_{42}	(kg)	108	ℓ_{32}	(m)	0.11	EI_2	(Nm²)	2.1E+7
J_{11}	(kgm²)	2.0	ℓ_4	(m)	2.37	EI_3	(Nm²)	1.0E+7
J_{12}	(kgm²)	2.8	ℓ_{41}	(m)	0.11	EI_4	(Nm²)	8.6E+6
J_{21}	(kgm²)	1.0	ℓ_{42}	(m)	0.39	k_1	(Nm/rad)	4.5E+6
J_{22}	(kgm²)	1.1	ℓ_5	(m)	0.77	k_2	(Nm/rad)	3.0E+6
J_{31}	(kgm²)	0.3	L_{C1}	(m)	0.80	k_3	(Nm/rad)	2.5E+6
Bucket								
m_{G2}	(kg)	1110	ℓ_{G2}	(m)	0.45	h_{G2}	(m)	0.80
J_{G2}	(kgm²)	250	ℓ_{C7}	(m)	0.11	h_{C7}	(m)	0.19
Cylinder								
A_{DC}	(m²)	1.6E-2	A_{PLG}	(m²)	1.3E-3	V_{LC0}	(m³)	2.3E-4
A_{LC}	(m²)	5.7E-3	V_{DC0}	(m³)	1.0E-3	K_{OIL}	(Pa)	1.4E+9

where k_{IX}^* is the equivalent spring constant of the derricking cylinder due to the compressibility of the working oil, d_{IX}^* is the distance from C_0 to the center line of the derricking cylinder, η_{C2} is the displacement of C_2, σ^* is the angle between the ξ axis and the center line of the derricking cylinder, u is the displacement of the plunger, and "*" denotes the quantity corresponding to the reference vector q^*.

(E) Upper leveling cylinder :

$$U_{LC} = \frac{1}{2} k_{LC}^* \left[d_{LC}^* (\gamma - \gamma^*) \right]^2 \tag{11}$$

where k_{LC}^* is the equivalent spring constant of the upper leveling cylinder, and d_{LC}^* is the distance from C_6 to the center line of the upper leveling cylinder.

3.2 Generalized forces

When the horizontal force F_x, the vertical force F_z and the moment of force M_{xz} are applied on the point G_2, the power done by these external forces becomes

$$W_{ext} = (F_x \sin\lambda + F_z \cos\lambda) v_{G2} + (F_x \cos\lambda - F_z \sin\lambda) w_{G2} + M_{xz} \dot{\psi} \tag{12}$$

By using the relation $\dot{q}^T Q = W_{ext}$, the generalized force vector $Q(q, F_x, F_z, M_{xz})$ is given by

$$Q(q, F_x, F_z, M_{xz}) = \partial W_{ext} / \partial \dot{q} \tag{13}$$

3.3 Equations of motion

Mechanical energies T, U and V in eq.(3) are written as the following form by neglecting the higher order terms with respect to $q - q^*$ and $\dot{q}$.

$$\left.\begin{aligned} T &= \frac{1}{2} \dot{q}^T M(q^*) \dot{q} \\ U &= \frac{1}{2} (q - q^*)^T D(q^*)(q - q^*) - (q - q^*)^T B(q^*) u \\ &\quad + (A_{PLG} / A_{DC})^2 u^2 \\ V &= V(q^*) - (q - q^*)^T G(q^*) \\ &\quad - \frac{1}{2} (q - q^*)^T E(q^*)(q - q^*) \end{aligned}\right\} \tag{14}$$

where M,D and E are symmetric matrices, B and G are vectors. As for the generalized force, it is approximated by using q^* instead of q. Therefore, the equations of motion given by the Lagrange's method becoms

$$\left.\begin{aligned} &M(q^*)\ddot{q} + \left[\dot{M}(q^*) + C(q^*)\right]\dot{q} + K(q^*)(q - q^*) \\ &\quad = G(q^*) + Q(q^*, F_x, F_z, M_{xz}) + B(q^*) u \end{aligned}\right\} \tag{15}$$

where

$$\left.\begin{aligned} K(q^*) &= D(q^*) - E(q^*) \\ C(q^*) &= \nu_M M(q^*) + \nu_K K(q^*) \end{aligned}\right\} \tag{16}$$

Since the damping matrix $C(q^*)$ is unknown, it is approximated by the proportional damping as shown in eq.(16), where ν_K and ν_M are determined so that the damping ratio of the 1st and 2nd mode vibrations coincide with their measurements.

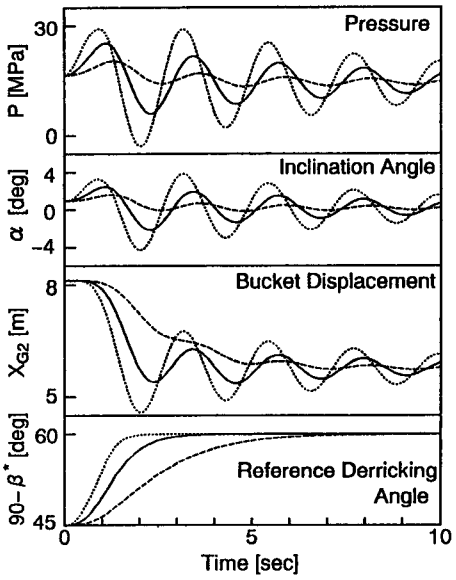

Fig.4 Free vibration caused by the change of reference derricking angle

4. Vibration Characteristics

4.1 Free vibration

Fig.4 shows the time history of the free vibrations of the pressure P in the derricking cylinder, the inclination angle α and the horizontal displacement x_{G2} of the bucket for the

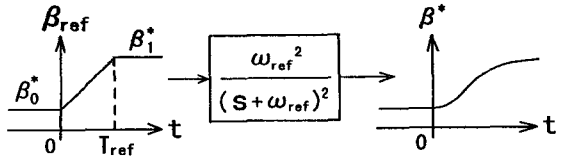

Fig.5 Generation of the reference derricking angle

change of the reference derricking angle $90°-\beta^*$. Three types of the reference derricking angles are used, which are shown in the bottom of Fig.4, where β^* is generated by using the procedure shown in Fig.5 with the parameters of T_{ref} = 1sec and $\omega_{ref} = 0.3\pi$, 0.7π and 1.5π rad/sec.

In this paper, in order to control the above mentioned vibration, the plunger attached to the derricking cylinder is used. In order to study the characteristics of this control system, the responses of pressure P, cylinder length a_{DC} and strain ε to the step change of u at $\beta^* = 45°$ are calculated and the results are shown in Fig.6. As seen from Fig.6, every one of P, a_{DC} and ε includes the higher mode vibration. Therefore, if these variables are fed back to u directly, instability will be caused, where ε is the strain of the boom at the point C_2, and defined by

$$\varepsilon = -1000 l_1 \left[\frac{d^2\eta}{d\xi^2}\right]_{\xi=l_{C2}} \tag{17}$$

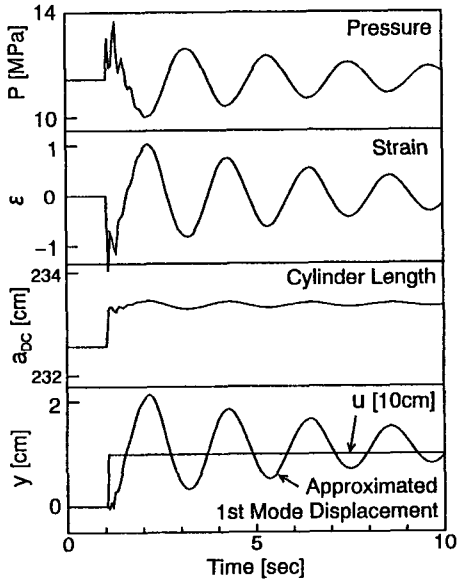

Fig.6 Response of P, ε and a_{DC} to the step change of u

4.2 Vibration modes

Consider the situation that β^*=constant. In this case, the vibration Δq of the aerial vehicles is described by

$$M(q^*)\Delta\ddot{q} + C(q^*)\Delta\dot{q} + K(q^*)\Delta q = B(q^*)u \tag{18}$$

and the solution is expressed as

$$\Delta q = W_1 v_1 + W_2 v_2 + \cdots + W_{16} v_{16} \tag{19}$$

where W_i ($i = 1\sim16$) is the vibration mode vector and v_i is the mode variable. W_i is given by

$$\left[-M(q^*)\omega_i^2 + K(q^*)\right]W_i = 0 \tag{20}$$

where ω_i is the natural angular frequency and the normalization is done by the following equation

$$\frac{1}{2}W_i^T K(q^*)W_i = E_0 \tag{21}$$

where E_0 is the elastic energy (about 3700J) of the static deformation due to the gravity force. On the other hand, using the orthogonality of the mode vectors, mode variable v_i is given by

$$v_i = \frac{g_i\omega_i^2}{s^2 + 2\zeta_i\omega_i s + \omega_i^2}u \tag{22}$$

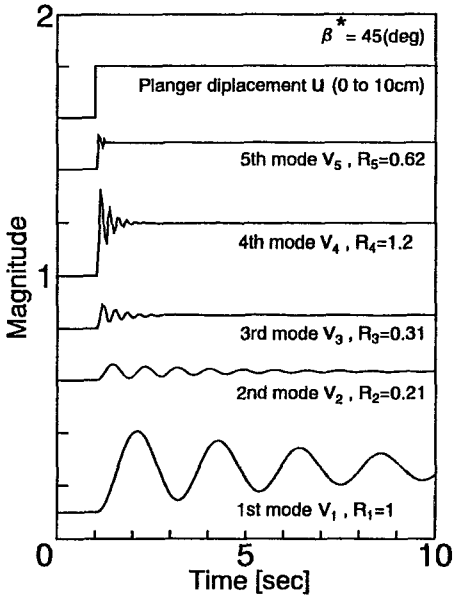

Fig.7 Response of mode displacements to the step change of u

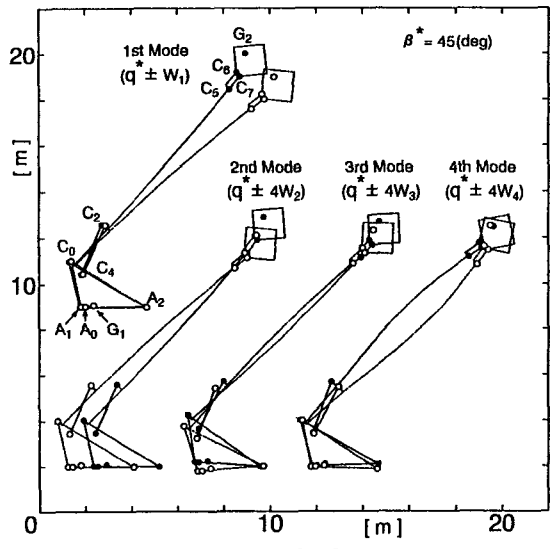

Fig.8 Mode shapes

where

$$\left.\begin{aligned} g_i &= \boldsymbol{W}_i^T \boldsymbol{B}(\boldsymbol{q}^*)/2E_0 \\ \varsigma_i &= (v_M/\omega_i + v_K\omega_i)/2 \end{aligned}\right\} \quad (23)$$

The response of the mode variables $v_1 \sim v_5$ to the step change of u are shown in Fig.7, and the shapes of the vibration modes $\boldsymbol{q}^* \pm \boldsymbol{W}_1$ and $\boldsymbol{q}^* \pm 4\boldsymbol{W}_i\,(i=2\sim4)$ are shown in Fig.8.

4.3 Detection of the 1st mode vibration

The detection of the 1st mode vibration is done by using the strain ε, because the ratio of the higher modes vibration to the 1st mode vibration is smallest for ε among the measurements of P, ε, a_{lX} shown in Fig.6. If eq.(17) is written as

$$\varepsilon = \boldsymbol{H}^T(\boldsymbol{q}^*)\Delta\boldsymbol{q} \quad (24)$$

then ε becoms as follows.

$$\left.\begin{aligned} \varepsilon &= \sum_{i=1}^{16} \frac{\lambda_i\omega_i^2}{s^2+2\varsigma_i\omega_i s+\omega_i^2}u \\ \lambda_i &= \boldsymbol{H}^T(\boldsymbol{q}^*)\boldsymbol{W}_i g_i \end{aligned}\right\} \quad (25)$$

Since $\lambda_1+\lambda_2+\cdots+\lambda_{16}=0$ for the strain, ε can be rewritten as follows.

$$\left.\begin{aligned} \varepsilon &= \frac{\lambda_1\omega_1^2}{s^2+2\varsigma_1\omega_1 s+\omega_1^2}u - \lambda_1 u + \sum_{i=1}^{16} n_i \\ n_i &= \lambda_i\left[\omega_i^2/\left(s^2+2\varsigma_i\omega_i s+\omega_i^2\right)-1\right]u \end{aligned}\right\} \quad (26)$$

Therefore the 1st mode displacement (the first term of eq.(26)) is approximated by

$$y = \varepsilon + \lambda_1 u - n_2 - n_3 - n_4 \quad (27)$$

The time history of y is shown in Fig.6, and it gives a good approximation of true 1st mode displacement v_1 shown in Fig.7.

5. Control law

5.1 Control low

The block diagram of the control system is shown in Fig.9, where the disturbance is the thing such as the change of the derricking angle, the external forces acted on the bucket and so on, $1/(1+T_a s)$ is the dynamic characteristic of the plunger driving device, v is the compensated input, $(1+T_L s)/(1+cT_L s)$ is the lag-element to smooth the input u. The saturation-element is used to prevent excessive inputs.

In order to derive the feedback control low, the dynamic characteristic from u_L to y in Fig.9 is approximated as follows.

$$y = \frac{\lambda_m\omega_m^2}{(1+T_m s)\left(s^2+2\varsigma_m\omega_m s+\omega_m^2\right)}(u_L+d) \quad (28)$$

where $T_m = T_a + (c-1)T_L$ is time constant, $(\lambda_m, \varsigma_m, \omega_m)$ is a set of approximated parameters of the 1st mode displacement, and d is the equivalent input disturbance.

As for the control strategy, u_L is designed so that the damping factor ς_m is replaced by larger value ς_P in the closed loop. From this point of view, the following controller is derived,

$$\left.\begin{aligned} u_L &= -g_1\hat{y} - g_2\hat{\dot{y}} \\ g_1 &= 2(\varsigma_P - \varsigma_m)/(\lambda_m\omega_m), \quad g_2 = g_1 T_m \end{aligned}\right\} \quad (29)$$

where $\hat{y}$ and $\hat{\dot{y}}$ is the estimates of the velocity and the acceleration of y, respectively. These estimates are obtained by using the following disturbance observer

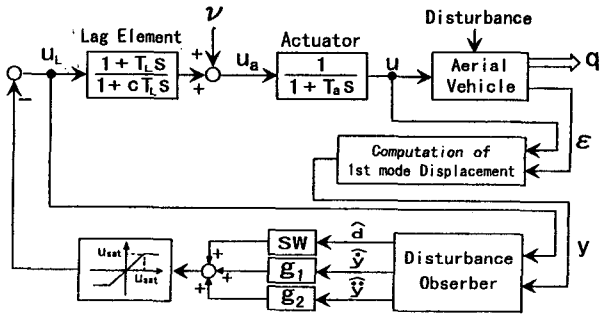

Fig.9 Block diagram of the control system

$$\frac{d}{dt}\begin{bmatrix}\hat{y}\\ \hat{\dot{y}}\\ \hat{\ddot{y}}\\ \hat{d}\end{bmatrix} = \begin{bmatrix}0 & 1 & 0 & 0\\ 0 & 0 & 1 & 0\\ -a_3 & -a_2 & -a_1 & a_0\\ 0 & 0 & 0 & 0\end{bmatrix}\begin{bmatrix}\hat{y}\\ \hat{\dot{y}}\\ \hat{\ddot{y}}\\ \hat{d}\end{bmatrix} + \begin{bmatrix}0\\ 0\\ a_0\\ 0\end{bmatrix}u_L + \begin{bmatrix}N_1\\ N_2\\ N_3\\ N_4\end{bmatrix}(y-\hat{y}) \quad (30)$$

where

$$\left.\begin{aligned} &a_0 = \lambda_m\omega_m^2,\ a_1 = 2\varsigma_m\omega_m + 1/T_m \\ &a_2 = \omega_m^2 + 2\varsigma_m\omega_m/T_m,\ a_3 = \omega_m^2/T_m \\ &N_1 = 4\omega_P - a_1,\ N_2 = 6\omega_P^2 - N_1 a_1 - a_2 \\ &N_3 = 4\omega_P^3 - N_2 a_1 - N_1 a_2 - a_3,\ N_4 = \omega_P^4/a_0 \end{aligned}\right\} \quad (31)$$

5.2 Stability of closed loop system

To investigate the stability of the control law, the root locus of the closed loop system of Fig.9 is plotted for $\omega_P = 3\sim10$rad/sec. The result is shown in Fig.10, where parameters are $T_a = 0.05$sec, $T_L = 0.03$sec, $c=6$, $\varsigma_P = 1.0$ and $\beta^* = 45°$.

The left hand side of Fig.10, Control(1), is the case that the correct values of the mode parameters $(\lambda_i, \varsigma_i, \omega_i)$, $i=1\sim4$

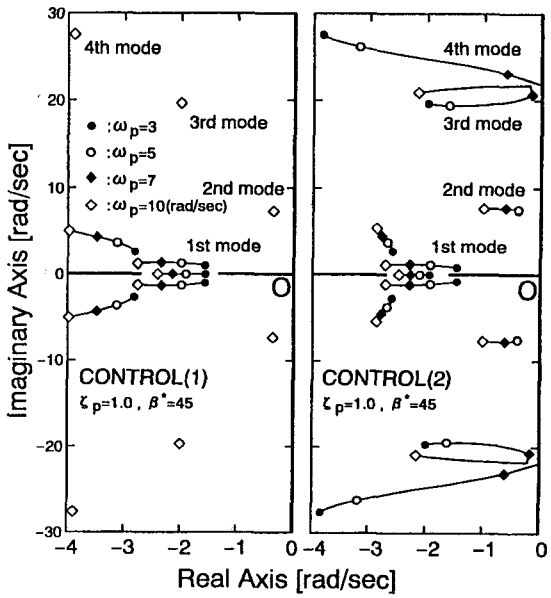

Fig.10 Root locus of the closed loop system, where Control(1) is eq.(27), Control(2) is eq.(32).

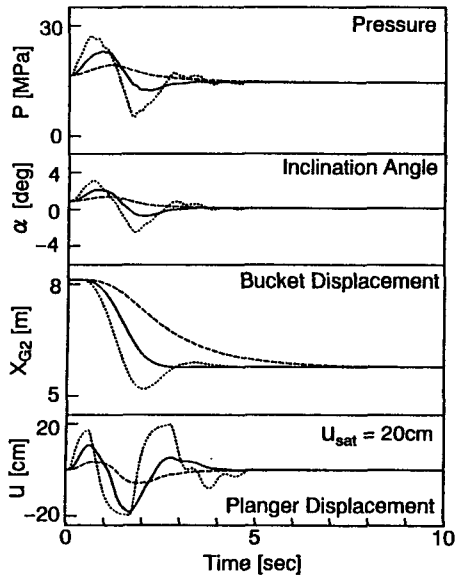

Fig.11 Control result corresponding to Fig.4

can be utilized. On the other hand, Control(2) is the case that only the 1st mode parameter can be utilized, and then y is computed by the following equation

$$y = \varepsilon + \lambda_1 u \tag{32}$$

6. Simulation

6.1 Change of the derricking angle

Fig.12 shows the result of the vibration control for the change of the derricking angle with the same condition as used in Fig.4. Fig.13 shows the result of the vibration control for the various derricking angles ($-20^\circ \sim 110^\circ$).

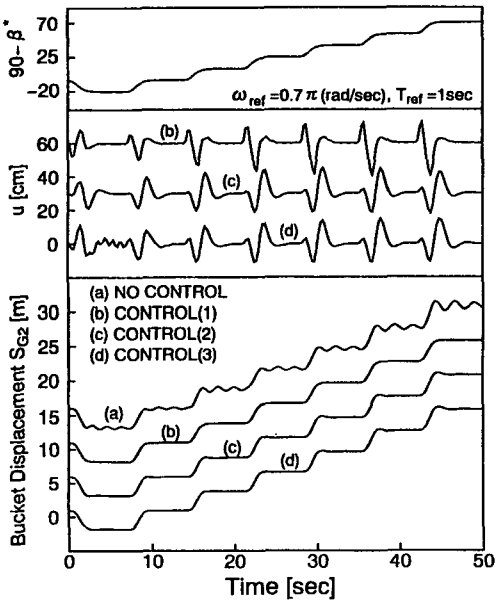

Fig.12 Control results for the various derricking angles, where the available information about the modal parameters becomes little in order of (b),(c),(d).

6.2 Wind force disturbance

Fig.14 shows the result of the vibration control when the wind blows against the bucket. The maximum speed of the wind is 15m/sec. The external forces due to the wind are given by $F_z = M_{xz} = 0$ and

$$F_x = \frac{1}{2}\rho C_D A_D v_D^2 \tag{33}$$

where ρ is the density of the air (1.226Kg/m^3), C_D is the coefficient of the wind force, A_D is the area perpendicular to the wind, and v_D is the wind velocity.

7. Conclusion

In this paper, an active vibration control scheme of aerial vehicles was proposed, and its effectiveness was confirmed by numerical simulations.

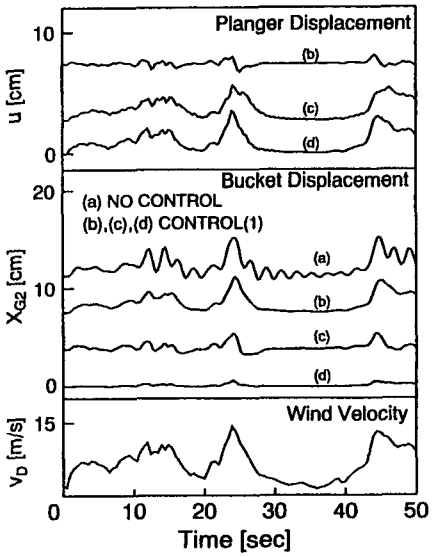

Fig.13 Control results for the wind force disturbance, where
(b) is the case of no compensation input(SW=0, $v = 0$),
(c) is the case of SW=1, $v = 0$,
(d) is the case of SW=0, $v = const. \times F_x$.

References

[1] S.Nio and Y.Maruyama: Remote-operated robotic system for live-line maintenance work, The Sixth Int. Conf. on transmission, Distribution Construction and Live-Line Maintenance, ESMO93, 425/435(1993)

[2] K.Konishi and H.Ukida: Active vibration control of aerial vehicles, SICE'96 in Tottori, 1135/1137 (1996)

[3] H.Ito, M.Hasegawa and H.Tada: A study on the dynamic behavior of truck crane with box type jibu(in Japanese), JSME, 52-475, 885/893(1986)

[4] T.Sakai, T.Arakawa, T.Yoshimura and T.Hino: Dynamic behavior of truck cranes in operation(in Japanese), JSME, 58-550, 1942/1949(1992)

[5] K.Konishi and H.Ukida: Modeling and Vibration Control of Aerial Vehicles, SICE'97 in Tokushima, 995/1000(1997)